

High Performance Micro CO Sensors Based on ZnO-SnO₂ Composite Nanofibers with Anti-Humidity Characteristics *

YUE Xue-Jun(岳学军)^{1,2}, HONG Tian-Sheng(洪添胜)¹, XIANG Wei(向伟)^{2**},
CAI Kun(蔡坤)¹, XU Xing(徐兴)¹

¹Key Laboratory of Key Technology on Agricultural Machine and Equipment (Ministry of Education), Engineering College, South China Agricultural University, Guangzhou 510642

²Faculty of Engineering and Surveying, University of Southern Queensland, Toowoomba QLD 4350, Australia

(Received 15 March 2012)

ZnO-SnO₂ composite nanofibers are synthesized via an electrospinning method and characterized by x-ray diffraction, scanning electron microscopy, and transmission electron microscopy. Micro sensors are fabricated by spinning the nanofibers on Si substrates with Pt signal and heater electrodes. The sensors with small areas (600 μm × 200 μm) can detect CO down to 1 ppm at 360 °C. The corresponding sensitivity, response time, and recovery time are 3.2, 6 s, and 11 s, respectively. Importantly, the sensors can operate at high humidity conditions. The sensitivity only decreases to 2.3 when the sensors are exposed to 1 ppm CO at 95% relative humidity. These excellent sensing properties are due to combining the benefits of one-dimensional nanomaterials and the ZnO-SnO₂ grain boundary in the nanofibers.

PACS: 07.07.Df, 82.47.Rs

DOI: 10.1088/0256-307X/29/12/120702

Inspired by their small volume, low power-consumption, excellent consistency and good compatibility, micro sensors have received considerable attention in recent decades.^[1] Micro sensors are usually fabricated by semiconducting techniques (such as thermal evaporation and reactive ion etching) and their areas range from several μm² to several mm².^[2] These characteristics make them good candidates for sensor integration, and therefore show potential applications in functional integrated circuits. Traditional micro sensors are based on metal-oxide semiconductor (MOS) sensing materials, which are normally synthesized by coating MOS pastes (via sol-gel), sputtering MOS targets (via direct-current or radio-frequency sputterings), or depositing MOS vapors (via metal organic chemical vapor deposition).^[3] However, the sensing films fabricated by these techniques are formed by compact nanoparticles, which often suffer from a degradation because of the aggregation growth among the nanoparticles.^[4,5] Especially, with the low thickness (only several μm) and high working temperatures (above 200 °C), the aggregation in the sensing films will constantly increase along work times.

In recent years, one-dimensional (1D) MOS nanomaterials have proved to be able to avoid such degradation.^[6] Simultaneously, the high surface-to-volume ratios of 1D nanomaterials can provide more sites for analyte molecules adsorption, leading to high sensitivities and short response/recovery times. Moreover, their large length-to-diameter values can also make charge carriers traverse the barriers introduced by molecular recognition as well.^[7] Many 1D MOS-related micro sensors have been frequently reported,^[8] however, most of them are only focused on low-toxicity gases such as C₂H₅OH, H₂, and CH₄. This is mainly

because it is hard for the practicalities (such as selectivity, anti-humidity, stability) of chemical sensors for toxic gases to satisfy the demand of applications.

CO is a kind of colorless, tasteless, widespread and toxic gas, which can be generated during the burning of fossil fuels and is produced by malfunctioning domestic appliances.^[9] Even at low concentrations (ppm level), well below immediately dangerous to life and health (IDLH) levels, it can have negative effects on human health. This highly toxic gas can attach to the haemoglobin, and damages the human body by producing a reduction in cellular respiration. Therefore, many scientists have performed a lot of works to tailor the performances of CO sensors. However, most of these sensors are based on nanoparticle materials, and the micro CO sensors with 1D nanomaterials are rarely reported.

In this Letter, we present micro sensors fabricated from ZnO-SnO₂ composite nanofibers. The sensors possess small area, high sensitivity, and quick response and recovery. In particular, they can also operate at various relative humidity (RH) conditions. Humidity interference is an important parameter for the practicality of gas sensors. Some sensors are even insensitive at high RH levels.^[10] The current sensors exhibit both high CO sensing performance and anti-humidity characteristics, which make them good candidates for the fabrication of practical CO sensors.

All chemicals (analytical grade reagents) were purchased from Beijing Chemicals Co. Ltd. and used as received without further purification. The electrospinning process in the present experiment is similar to those described previously for metal oxide nanofiber synthesis.^[11,12] Typically, an appropriate amount of SnCl₂·2H₂O was mixed with the 1:1 weight ratio of N,

*Supported by the Special Fund for Agro-scientific Research in the Public Interest of China (No 200903023), Science and Technology Projects in Guangdong Province (2010B020314007), and the Cooperation Projects of Industry, Education and Academy Sponsored by Guangdong Province and Ministry (2011B090400359).

**Corresponding author. Email: xiangweiaustralia@gmail.com

© 2012 Chinese Physical Society and IOP Publishing Ltd

N-dimethylformamide (DMF) and ethanol in a glove-box under vigorous stirring for 10 min. Then, this solution was in turn added into 0.8 g of poly (vinyl pyrrolidone) (PVP, molecular weight 1.3×10^6) and the suitable amount of zinc acetate aqueous solution (0, 0.5wt%, 1wt%, 1.5wt%) under vigorous stirring for 6 h. The mixture obtained was delivered to a hypodermic syringe at a constant flow rate of 1.0 mL/h, and then electrospun by applying 17 kV at an electrode distance of 20 cm. A piece of flat aluminum foil was employed to collect the precursory jets.

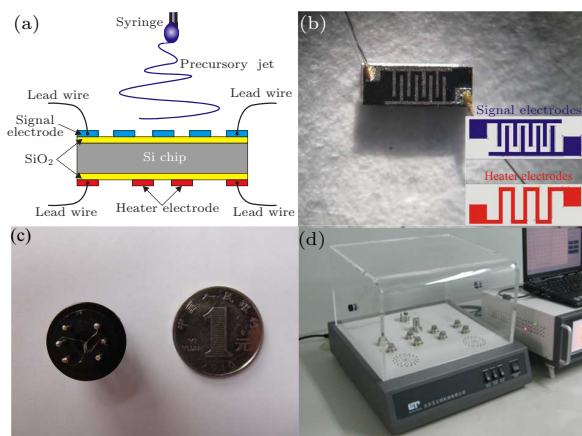


Fig. 1. (a) Fabricating process of ZnO-SnO₂ micro sensors, (b) a photograph of sensor substrates and its electrode design, (c) comparison between a socketed sensor and a Chinese coin (1 Yuan), and (d) a photograph of the sensing analysis system with eight micro sensors in it.

ZnO-SnO₂ micro sensors were fabricated by spinning ZnO-SnO₂ composite nanofibers on sensor substrates (Fig. 1(a)). The substrates were achieved according to the following steps: (a) growth of SiO₂ (thickness of 2000 Å) on the two sides of Si-substrates as insulating layer, (b) sputtering platinum (thickness of 1800 Å) on SiO₂ layers as metal electrodes, (c) mask patterns transfer to the Si wafer by photolithography, (d) etching the platinum layers to form signal electrodes and heater electrodes by reactive ion etching, (f) removing the photoresist. A top view (obtained in a microscope) and the electrode design of the micro sensors are shown in Fig. 1(b). The electrode width was 20 μm, and the sensor area was 600 μm × 200 μm. Sensing films were obtained by laying sensor substrates on the aluminum foil in the electrospinning process, and spinning ZnO-SnO₂ precursory jets for 4 h. Then the substrates were calcined at 600°C for 3 h to remove PVP and convert precursory jets to ZnO-SnO₂ composite nanofibers. Figure 1(c) shows a comparison between a socketed micro sensor and a Chinese coin.

The sensor performances were measured by a CGS-8 (Chemical Gas Sensor-8) intelligent gas sensing analysis system (Beijing Elite Tech Co., Ltd, China) (Fig. 1(d)). This system could provide various operating currents to control the sensor temperature (measured by a Testo 845 infrared thermometer (TESTO AG, Germany)). Gas ambiances were obtained by a static test system. All the sensors were pre-heated

at different operating temperatures for about 30 min. When the resistances of the sensors were stable, saturated target gas was injected into the test chamber (20 L in volume) by a micro-injector through a rubber plug. The saturated target gas was mixed with air by two fans in the analysis system. After the sensor resistances reached new constant values, the test chamber was opened to recover the sensors in air. The whole experiment process was performed in a super-clean room with the constant humidity (25% RH) and temperature (20°C) (which were also monitored by the analysis systems). The humidity interference of the sensors was studied by exposing them to a mixed gas, which was prepared by filling CO of known concentrations into the chambers with different RH levels. The RH ambiances of 54% RH (corresponding to Mg(NO₃)₂) and 95% RH (corresponding to KNO₃) were obtained using saturated salt solutions as the humidity generation sources.

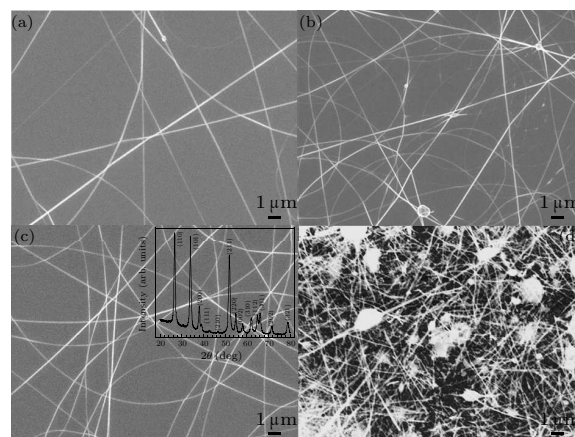


Fig. 2. SEM images of (a) SnO₂, (b) 0.5wt% ZnO-SnO₂, (c) 1wt% ZnO-SnO₂, and (d) 1.5wt% ZnO-SnO₂ nanofibers. The insert in (c) shows the XRD pattern of the 1wt% ZnO-SnO₂ composite nanofibers.

The response value R was designated as $R = R_a/R_g$, where R_a is the sensor resistance in air (base resistance) and R_g is of a mixture of target gas and air. The time taken by the sensor resistance to change from R_a to $R_a - 90\% \times (R_a - R_g)$ was defined as response time when the target gas was introduced to the sensor, and the time taken from R_g to $R_g + 90\% \times (R_a - R_g)$ was defined as recovery time when the ambience was replaced by air.

The crystal structures of the products were determined by x-ray powder diffraction (XRD) using an x-ray diffractometer (Siemens D5005, Munich, Germany). The morphologies of the electrospun nanofibers were viewed by scanning electron microscopy (SEM, SSX-550, Shimadzu). Transmission electron microscopy (TEM) images were obtained on a HITACHI H-8100 microscope using an acceleration voltage of 200 keV.

Figures 2(a), 2(b), 2(c), and 2(d) show the SEM images of the obtained SnO₂ and ZnO-SnO₂ (0.5wt%, 1wt%, 1.5wt%) composite nanofibers, respectively. The samples are highly dominated by nanofibers with lengths of several tens of micrometer and diameters

ranging from 60 to 120 nm. An aggregate phenomenon is observed with higher ZnO contents (Fig. 2(d)), which is because Sn and Zn have different electrical density (+4 and +2 respectively), and this can affect the electrospinning condition for the nanofibers. The insert in Fig. 1(c) displays the XRD pattern of the 1wt% ZnO-SnO₂ composite nanofibers. The prominent peaks corresponding to (110), (101) and (211) crystal lattice planes and all other smaller peaks coincide with the corresponding peaks of the rutile structure of SnO₂ given in the standard data file (JCPDS File No41-1445). No diffraction peaks corresponding to ZnO can be observed, which is because ZnO is highly solved in SnO₂. The XRD results of other samples (0, 0.5wt%, and 1.5wt% ZnO-SnO₂ nanofibers) are similar to that in the insert of Fig. 2(c).

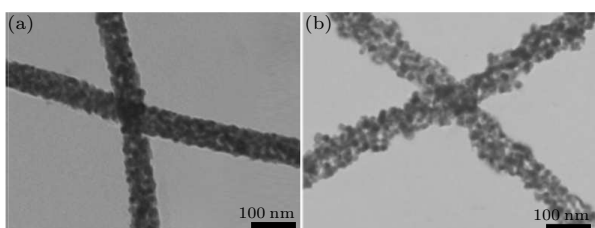


Fig. 3. TEM images of (a) SnO₂ and (b) ZnO-SnO₂ composite nanofibers.

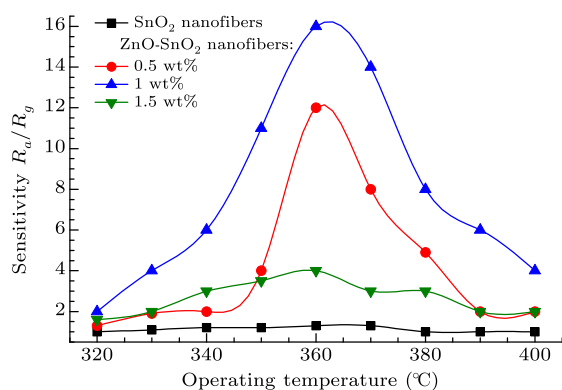


Fig. 4. The sensor sensitivities to 100 ppm CO at different working temperatures.

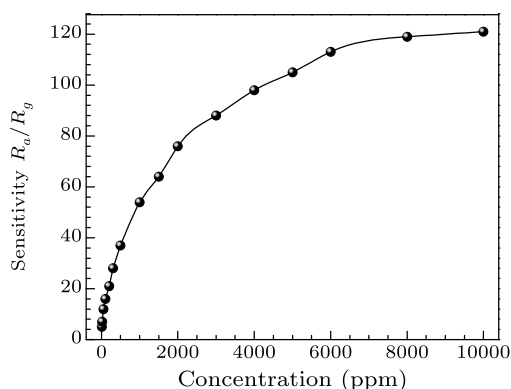


Fig. 5. The sensor sensitivities to different CO concentrations at 360°C.

To reveal the morphological infection of ZnO in SnO₂ nanofibers, TEM analyses were performed. The resultant images of SnO₂ nanofibers and 1wt% ZnO-

SnO₂ composite nanofibers are shown in Fig. 3. After adding ZnO in SnO₂ nanofibers, the fibers become much coarser and some clinging nanoparticles are found. These morphological characteristics are beneficial for the gas adsorption,^[13] thus may lead to a high sensing performance eventually.

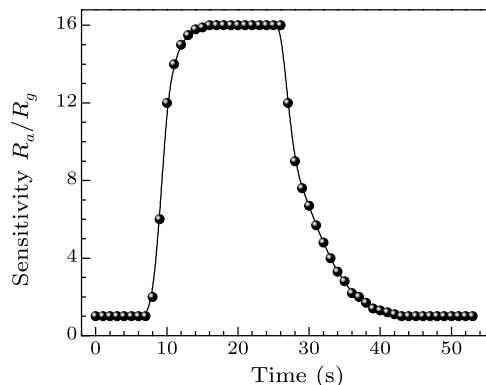


Fig. 6. Response and recovery characteristics of the sensors to 100 ppm CO at 360°C.

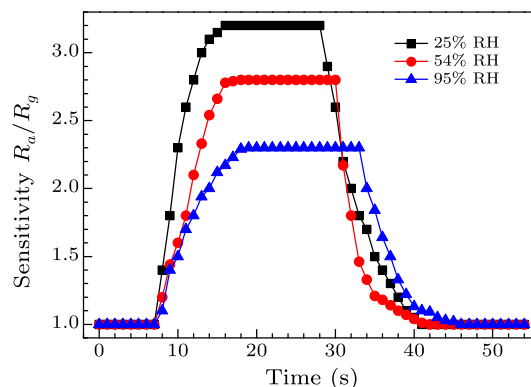


Fig. 7. Response and recovery characteristics of the sensors to 100 ppm CO at different RH conditions.

The fabricated micro sensors are exposed to 100 ppm CO at various temperatures to find the optimized working conditions. As shown in Fig. 4, all the samples exhibit response to CO, but their sensitivities are quite different. SnO₂ nanofiber sensors only show a very low sensitivity (about 1.1), while ZnO-SnO₂ nanofiber sensors possess much higher sensitivity. The highest sensitivity of about 16 is obtained from the sensors with 1wt% ZnO-SnO₂ composite nanofibers at 360°C. The much higher sensitivity directly proves the sensing benefit of ZnO in SnO₂ nanofibers. The decreased sensitivity of 1.5wt% ZnO-SnO₂ composite nanofibers is due to the aggregate nanofibers of this sample. Therefore, all the tests below were focused on 1wt% ZnO-SnO₂ nanofiber sensors and performed at 360°C (the optimized temperature).

The micro sensor sensitivity versus CO concentration at 360°C is shown in Fig. 5. The sensors can detect CO down to 1 ppm, and the corresponding sensitivity is about 3.2. With rising CO concentration, the sensor sensitivity rapidly increases. For instance, the sensitivities are about 5, 16, and 54 to 10, 100, and 1000 ppm CO. The sensors reach saturation at about 8000 ppm (the sensitivity is about 120). These results

indicate that the presented sensors are more suitable for CO detection at low concentrations.

Figure 6 shows the sensitivity versus time curve of the micro sensors at 360°C. The CO concentration used in this test was 100 ppm. As can be seen in the response-recovery curve, the response and recovery times are about 6 and 11 s, respectively, which are much shorter than those of many reported CO sensors.^[9] This quick reaction is based on the 1D nanostructure of the nanofibers, and the theoretical explanation is shown in the discussion section.

Figure 7 shows the response-recovery curves of the micro sensors at different RH conditions. To find the detecting limit, the CO concentration was changed to 1 ppm. From Fig. 7, we can obtain that the sensitivity decreases when the RH is increased. However, the micro sensor can well detect 1 ppm CO in all the tests. Even in 95% RH, the sensitivity is about 2.3, indicating the anti-humidity characteristics of the presented sensors.

Furthermore, the micro sensors were also exposed to different gases (100 ppm) to reveal their selectivity at 360°C. The sensors show prominent sensitivity to CO, very low sensitivities to C₂H₅OH and CH₃OHCH₃, and almost no responses to CH₃OH, NH₃, C₆H₅CH₃, C₆H₆, CH₄, H₂ and C₂H₂. These results suggest that the sensors own a high selectivity and can be employed in various applications.

A possible CO sensing mechanism for ZnO-SnO₂ composite nanofibers is depicted as follows. The response between MOS sensing materials and reducing gases is mainly based on the interaction of the gas molecules and oxygen ions (O₂⁻, O⁻ and O²⁻).^[14] When the ZnO-SnO₂ composite nanofibers are exposed to air, the nanofiber surface will absorb some oxygen molecules, which can capture electrons from the conductance band of the nanofibers to become oxygen ions. At low temperatures, O₂⁻ is chemisorbed, while at high temperatures, O²⁻ and O are chemisorbed, and the O₂⁻ disappears rapidly. Therefore, the sensor resistance in ambient air is higher than that in a vacuum. When the nanofibers are exposed to CO, CO molecules will react with oxygen ions. The previous papers have discussed that the dominant oxygen ion in the sensing reaction is O.^[4,15] Therefore, the reaction can be simply written as



The electrodes released from the surface reaction transfer back into the conductance band, which can effectively decrease the sensor resistance.

The high CO sensitivity and excellent selectivity are directly related to the ZnO addition. The XRD result reveals that the ZnO does not change the crystal structure of the SnO₂ nanofibers at this doping ratio. However, the affected morphology of the nanofibers in TEM images implies that ZnO has changed the electrospinning state. This effect will lead to more absorbing sites on the nanofibers, and

also produce ZnO-SnO₂ contacts simultaneously.^[16] Ji and Choi have provided a hetero-contact mechanism to understand the high CO sensing properties of ZnO-SnO₂ systems.^[16,17] It was described that ZnO-SnO₂ grain boundary (in SnO₂ rich conditions), which is formed by these two n-type sensing materials, can greatly enhance the CO sensing properties, and thus contribute to high CO sensitivities. On the other hand, the ZnO-SnO₂ grain boundary formed in the sensing materials will also enhance their optimized temperature for CO detection (such as 360°C in this case), and lead to a much higher working temperature than other SnO₂ based sensors (normally about 300°C).^[18] The higher temperature can decrease the sensor sensitivity to many interferential gases such as C₂H₅OH and H₂O, which results in the high selectivity and anti-humidity characteristics. Moreover, the high sensitivity and quick response/recovery of the ZnO-SnO₂ composite nanofibers also have some relationships with the nanostructure of ZnO-SnO₂ composite nanofibers. The high density of surface sites and large surface-to-volume ratios brought about by their 1D nanostructures and coarse morphology can effectively promote the gas absorption on the sensor surface.^[9] Furthermore, the fabricating process for our sensors is scatheless for fiber morphology because no grinding and coating processes are used.^[11] Eventually, all these factors associatively lead to the high CO sensing properties of the ZnO-SnO₂ nanofiber micro sensors.

In summary, ZnO-SnO₂ composite nanofibers are synthesized through an electrospinning method. Micro sensors are fabricated by spinning the nanofibers on Si-based substrates. Excellent CO sensing properties are observed such as high sensitivity, quick response and recovery, and good selectivity. The sensors also show anti-humidity properties in the tests. The sensing mechanism is theoretically explained.

References

- [1] Nlta T 1981 *Ind. Eng. Chem. Prod. Res. Dev.* **20** 669
- [2] Lee S M et al 2003 *Microelectron. J.* **34** 115
- [3] Liu Y G et al 2007 *Appl. Phys. Lett.* **90** 042109
- [4] Liu L et al 2009 *Chin. Phys. Lett.* **26** 090701
- [5] Qiu C J et al 2008 *Chin. Phys. Lett.* **25** 3590
- [6] Kolmakov A and Moskovits M 2004 *Annu. Rev. Mater. Res.* **34** 151
- [7] Franke M E, Koplin T J and Simon U 2006 *Small* **2** 36
- [8] Xu L, Wang R, Xiao Q, Zhang D and Liu Y 2011 *Chin. Phys. Lett.* **28** 070702
- [9] Greiner A and Wendorff J H 2007 *Angew. Chem. Int. Ed.* **46** 5670
- [10] Qi Q et al 2008 *Sens. Actuat. B* **133** 638
- [11] Xu L et al 2011 *Chin. Phys. Lett.* **28** 040701
- [12] Li D and Xia Y 2004 *Adv. Mater.* **16** 1151
- [13] Qiao J P et al 2012 *Chin. Phys. Lett.* **29** 020701
- [14] Narsan N et al 2007 *Sens. Actuat. B* **121** 18
- [15] Varghese O K et al 2003 *Adv. Mater.* **15** 624
- [16] Ji H Y and Choi G M 1999 *Sens. Actuat. B* **61** 59
- [17] Ji H Y and Choi G M 1998 *Sens. Actuat. B* **52** 251
- [18] Chakraborty S et al 2006 *Sens. Actuat. B* **115** 610